Wang et al. *Zool. Res.* 2024, 45(5): 1013−1026
https://doi.org/10.24272/j.issn.2095-8137.2024.050
https://cstr.cn/32248.14.zr.2024.050

ZR | Zoological Research

Article Open Access

Comparative DNA methylation reveals epigenetic adaptation to high altitude in snub-nosed monkeys

Ling Wang[1,2,#], Wei-Qiang Liu[1,2,#], Juan Du[1], Meng Li[1], Rui-Feng Wu[1], Ming Li[1,3,*]

[1] *Key Laboratory of Animal Ecology and Conservation Biology*, *Institute of Zoology*, *Chinese Academy of Sciences*, *Beijing* 100101, *China*
[2] *University of Chinese Academy of Sciences*, *Beijing* 100049, *China*
[3] *Center for Excellence in Animal Evolution and Genetics*, *Chinese Academy of Sciences*, *Kunming*, *Yunnan* 650223, *China*

ABSTRACT

DNA methylation plays a crucial role in environmental adaptations. Here, using whole-genome bisulfite sequencing, we generated comprehensive genome-wide DNA methylation profiles for the high-altitude Yunnan snub-nosed monkey (*Rhinopithecus bieti*) and the closely related golden snub-nosed monkey (*R. roxellana*). Our findings indicated a slight increase in overall DNA methylation levels in golden snub-nosed monkeys compared to Yunnan snub-nosed monkeys, suggesting a higher prevalence of hypermethylated genomic regions in the former. Comparative genomic methylation analysis demonstrated that genes associated with differentially methylated regions were involved in membrane fusion, vesicular formation and trafficking, hemoglobin function, cell cycle regulation, and neuronal differentiation. These results suggest that the high-altitude-related epigenetic modifications are extensive, involving a complete adaptation process from the inhibition of single Ca^{2+} channel proteins to multiple proteins collaboratively enhancing vesicular function or inhibiting cell differentiation and proliferation. Functional assays demonstrated that overexpression or down-regulation of candidate genes, such as *SNX10*, *TIMELESS*, and *CACYBP*, influenced cell viability under stress conditions. Overall, this research suggests that comparing DNA methylation across closely related species can identify novel candidate genomic regions and genes associated with local adaptations, thereby deepening our understanding of the mechanisms underlying environmental adaptations.

Keywords: Snub-nosed monkeys; Whole-genome bisulfite sequencing; DNA methylation; High-altitude adaptation

INTRODUCTION

As the most extensively studied and best understood form of epigenetic modification, DNA methylation is known to play important roles in various biological processes, including transposable element silencing, gene expression regulation, genomic imprinting, X-chromosome inactivation, carcinogenesis, and aging (Bird, 2002; Horvath et al., 2022; Schübeler, 2015; Smith & Meissner, 2013). In mammals, DNA methylation predominantly occurs at the C-5 position of cytosine within CpG dinucleotides through the addition of a methyl group (Lisanti et al., 2013; Mohn & Schübeler, 2009). The function of DNA methylation varies depending on its genomic location. For example, DNA methylation in promoter regions is typically associated with gene repression, while gene-body DNA methylation is positively correlated with transcriptional activity (Ball et al., 2009; Jones, 2012; Lister et al., 2009).

Environmentally induced epigenetic changes may be inheritable (Jirtle & Skinner, 2007; Richards, 2006). Epigenetic modifications, particularly DNA methylation, can contribute to rapid phenotypic changes by modulating gene-regulatory responses to environmental conditions (Feil & Fraga, 2012). With the advancement of high-throughput sequencing and various assays for measuring DNA methylation, recent studies have elucidated the significant impact of DNA methylation on environmental adaptations. For instance, brown anole lizards (*Anolis sagrei*) exhibit consistent changes in DNA methylation within a few days of colonizing novel environments (Hu et al., 2019). In pigs (*Sus scrofa*), comparative methylated DNA immunoprecipitation sequencing has revealed differentially methylated genes potentially related to hypoxic adaptation between Xizang and Yorkshire pigs (Zhang et al., 2019). In humans, methylation of the promoter region of *EPAS1* and the repetitive element LINE-1is associated with differential exposure to high altitude (Childebayeva et al., 2019, 2021). These findings suggest that the role of epigenetic modifications, especially DNA methylation, in environmental

Received: 17 February 2024; Accepted: 25 April 2024; Online: 26 April 2024

Foundation items: This work was supported by the National Natural Science Foundation of China (32330015, 31821001) and Strategic Priority Research Program of the Chinese Academy of Sciences (XDB31000000)

[#]Authors contributed equally to this work

*Corresponding author, E-mail: lim@ioz.ac.cn

adaptations is greater than previously anticipated and merits thorough investigation (Bossdorf et al., 2008).

Whole-genome bisulfite sequencing (WGBS) is a standard approach for DNA methylation profiling (Chapin et al., 2022; Ulahannan & Greally, 2015), involving random genome fragmentation followed by bisulfite sequencing, thus providing nucleotide-resolution and comprehensive information on most cytosine locations across the genome (Susan et al., 1994; Suzuki et al., 2018). Notably, WGBS has enabled exploration of the role of DNA methylation in environmental adaptation at the genomic scale by comparing whole-genome DNA methylation profiles. For example, coral (*Stylophora pistillata*) exposed to varying pH stress exhibits widespread DNA methylation changes in pathways governing the cell cycle and body size, suggesting that an epigenetic component of phenotypic acclimatization may enable coral to better withstand environmental alterations (Liew et al., 2018). Similarly, as revealed by comparative analysis of genomic-scale DNA methylation, Chinese indigenous chickens (*Gallus domesticus*) under different conservation programs exhibit local genetic and DNA methylation variations associated with the environmental characteristics of their origin (Zeng et al., 2022).

The snub-nosed monkeys (genus *Rhinopithecus*) encompass five endangered and critically endangered colobine primate species distributed across China (*R. roxellana*, *R. brelichi*, *R. bieti*, and *R. strykeri*), Myanmar (*R. strykeri*), and Vietnam (*R. avunculus*) (Geissmann et al., 2011; Li et al., 2004). Among these species, the Yunnan snub-nosed monkey (*R. bieti*) uniquely inhabits high-altitude forests at elevations ranging from 3 400 to 4 600 m above sea level on the Qinghai-Xizang Plateau, representing one of the highest altitudinal ranges for nonhuman primates (Li et al., 2002; Long et al., 1994, 1996). In contrast, their close relatives, the golden snub-nosed monkey (*R. roxellana*), are confined to mountain forests in central China, typically at elevations below 3 300 m (Kirkpatrick, 1995).

Exploring genetic adaptations to high-altitude environments, Yu et al. (2011) found that mitochondrial genes in the golden snub-nosed monkey are under positive selection, potentially enhancing energy metabolism at high altitudes and in cold climates. Zhou et al. (2014) generated genomic sequences of snub-nosed monkeys and discovered positive selection of certain genes related to fatty acid biosynthesis and the signaling of insulin, adipocytokine, and lipid binding. They hypothesized that leaf-eating monkeys living in high-altitude forests evolved enhanced energy metabolism to efficiently degrade plant cell wall components (celluloses and hemicelluloses) and absorb and exploit scarce nutrients. In subsequent population genomic analyses, Zhou et al. (2016) identified positive selection signatures in several genes, including *ADAM9* and *SLC9A6*, within the Yunnan snub-nosed monkey genome that may facilitate adaptive responses to low oxygen conditions. Yu et al. (2016) also reported the selection of genes associated with DNA repair, DNA damage response, and oxidative phosphorylation in snub-nosed monkeys, potentially linked to increased ultraviolet (UV) exposure and higher metabolic rates required for survival at high altitudes. Despite their valuable role as a research model, the extent to which epigenetic modifications contribute to the complex adaptation of snub-nosed monkeys to high-altitude environments remains uncertain.

In this study, we generated genome-wide DNA methylation profiles for both Yunnan snub-nosed monkeys and golden snub-nosed monkeys using WGBS. We then conducted a population-level comparison of these profiles to determine whether the two species exhibit similar DNA methylation patterns characteristic of high-altitude environments. Additionally, we analyzed differentially methylated genomic regions and genes between the two species to investigate their potential role in high-altitude adaptation. Collectively, the findings of this study provide novel insights into the epigenetic mechanisms underlying the adaptation of snub-nosed monkeys to high-altitude environments.

MATERIALS AND METHODS

Sample collection, DNA isolation, and sequencing

Muscle samples were obtained from 15 snub-nosed monkeys, including 11 golden snub-nosed monkeys and four Yunnan snub-nosed monkeys, which died of natural causes in nature reserves. Information on their respective altitudinal habitats was also collected (Figure 1A, B; Supplementary Table S1). Genomic DNA was extracted from the muscle samples using a TIANamp Blood/Tissue/Cell Genomic DNA Extraction Kit DP304 (TIANGEN Biotech, China). The samples were first treated to create a cell suspension, then centrifuged at 10 000 r/min with a centrifugal radius of 8 cm for 1 min at 4 °C. The supernatant was discarded, and the cell pellet was re-suspended in 200 μL of Buffer GA. After the addition of 4 μL of RNase A (TransGen Biotech, China), the samples were incubated with 20 μL of Proteinase K (TransGen Biotech, China) at 56 °C until complete cell lysis. Subsequent steps were performed according to the manufacturer's instructions (DP304 TIANamp Genomic DNA Kit, TIANGEN Biotech, China). Approximately 5.2 μg of genomic DNA spiked with 26 ng of lambda DNA was fragmented to 200–300 bp with a Covaris S220 sonicator (Covaris, USA), followed by end repair and adenylation. Lambda DNA served as an unmethylated control to calculate the bisulfite conversion rate. The DNA fragments were then treated twice with bisulfite using an EZ DNA Methylation-Gold™ Kit (Zymo Research, USA). After testing the insert size and accurately quantifying the effective concentration of the libraries using real-time quantitative polymerase chain reaction (qPCR), the libraries were sequenced on the Illumina NovaSeq 6000 platform (Novogene, China), generating 150 bp paired-end reads. All study procedures and protocols were approved by the Animal Ethics Committee of the Institute of Zoology, Chinese Academy of Sciences (IOZ20190083, 26 December 2019).

Comparative WGBS data analysis

The NGS QC Toolkit v.2.3.3 (Patel & Jain, 2012) was used to remove low-quality reads and those containing adapters. Clean reads for each sample were mapped to the reference genome Rrox_v1 (GCF_000769185.1) using Bismark v.0.22.1 with default parameters (Krueger & Andrews, 2011). Duplicate reads were removed based on coordinates. Methylcytosine information was processed using the R package methylKit v.1.12.0 (Akalin et al., 2012). Bases with less than 10× coverage and those with more than 99.9% coverage in each sample were discarded to eliminate PCR bias (Supplementary Tables S2–S4). Coverage normalization was achieved by calculating the scaling factor using the median coverage for each sample. The genome was tiled with 1 000 bp windows and 1 000 bp step-size to summarize methylation information,

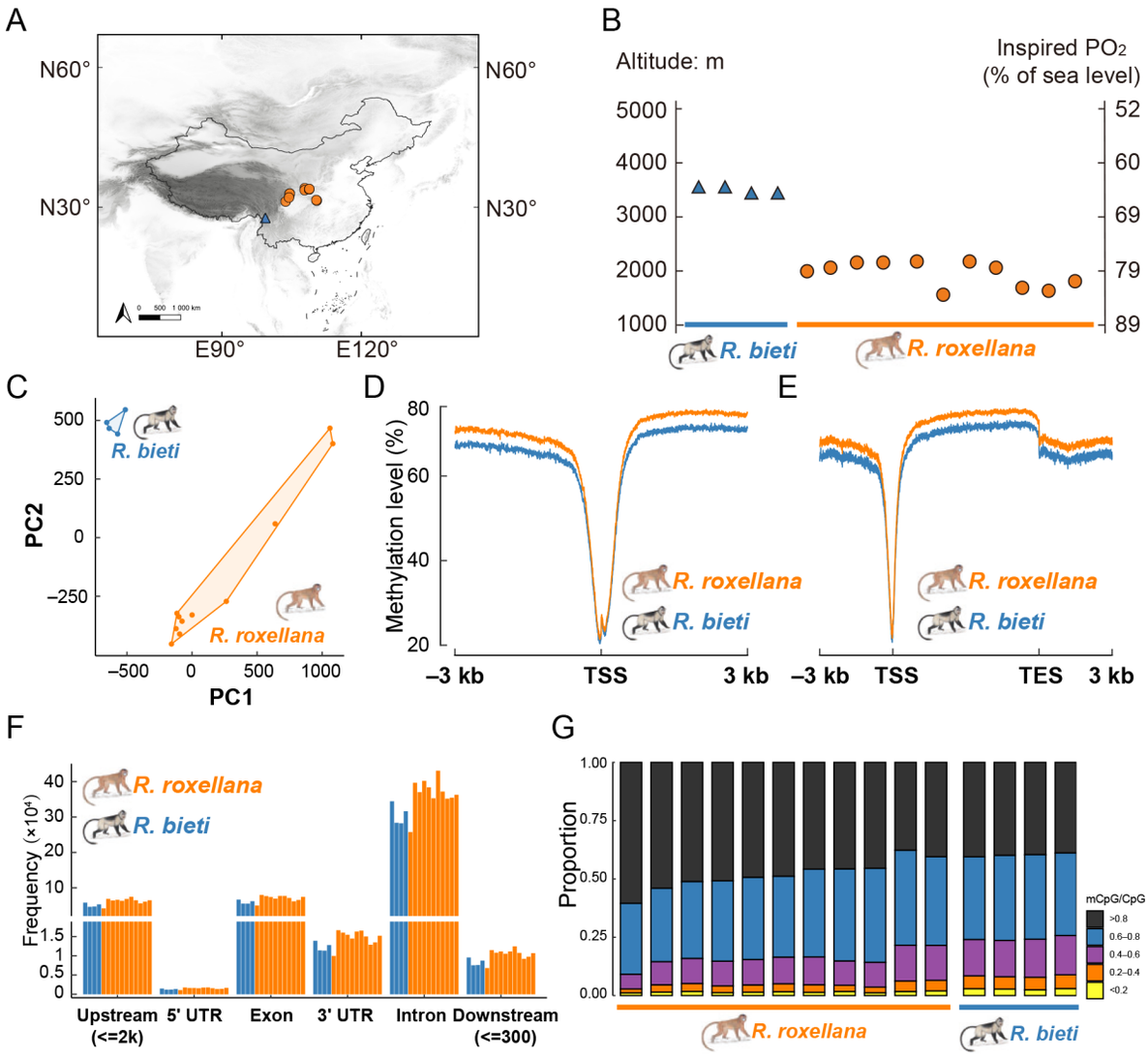

Figure 1 Sample and genomic methylation information related to snub-nosed monkeys

A: Study sampling sites in China. B: Altitude and oxygen partial pressure of each sampling location. Orange solid circle represents sampling locations of golden snub-nosed monkeys (*Rhinopithecus roxellana*) and blue triangle represents sampling locations of Yunnan snub-nosed monkeys (*R. bieti*). C: PCA of DNA methylation level across samples. First two principal components (PCs) are shown. Each sample is represented as a point. Colors represent golden snub-nosed monkeys (*R. roxellana*, orange) and Yunnan snub-nosed monkeys (*R. bieti*, blue). D: CG methylation distribution around transcription start sites (TSS) over Ensembl genes and 3k bp flanking sequences in the 1k bp region of golden snub-nosed monkeys (*R. roxellana*, orange) and Yunnan snub-nosed monkeys (*R. bieti*, blue). E: CG methylation distribution around the TSS and transcription end site (TES) over Ensembl genes and 3k bp flanking sequences in the 1k bp region of golden snub-nosed monkeys (orange) and Yunnan snub-nosed monkeys (blue). F: Frequency of hypermethylation sites (methylation rate >70% and coverage >30×) in gene upstream 2k bp, 5' UTR, exon, 3' UTR, intron, and gene downstream 300 bp. Colors represent golden snub-nosed monkeys (orange) and Yunnan snub-nosed monkeys (blue). G: Proportions of methylated CG sites. Color represents different methylation ratio ranges.

filtering regions with coverage lower than 3×. Principal component analysis (PCA) of DNA methylation levels across samples was conducted to identify any outliers among the samples from each species. The differentially methylated region (DMR) was identified by considering genomic area with an average methylation discrepancy greater than 25% and a *Q*-value below 0.01. Genes with DMRs extending within ±2 000 bp from the transcription start site (TSS) were classified as differentially methylated genes (DMGs). To ensure that variations in DMGs were not due to random variability or unequal sample sizes, strategic subsampling and repeated significance testing were implemented for each DMG. Given the computational intensity of random sampling, a semi-random approach was adopted. The samples were first clustered based on their methylation profiles using the "ward.D2" method (Supplementary Figure S1). The sample size of the golden snub-nosed monkeys was then matched to that of the Yunnan snub-nosed monkeys by drawing from each cluster of the former. Hence, 48 unique combinations were devised from the golden snub-nosed monkey clusters, ensuring systematic inclusion of all samples. For each gene, the highest *P*-value (denoting the least significance) and the corresponding methylation differential were recorded as the benchmark for significance.

Given that our analysis revealed higher methylation levels in golden snub-nosed monkeys compared to Yunnan snub-nosed monkeys, the same cutoff was not universally applied to identify significant DMGs. Instead, regions showing more

than a 40% methylation increase in golden snub-nosed monkeys were classified as hypermethylated, while those with a decrease of more than 10% were defined as hypomethylated. Regions with *Q*-value below 0.05 in comparative groups were designated as DMGs. To mitigate potential bias from exclusively using the golden snub-nosed monkey genome, the Yunnan snub-nosed monkey genome (GCA_001698545.1) was also employed in mapping and comparative analyses. Ultimately, DMGs demonstrating significant differences in both genome analyses were confirmed as definitive candidate genes.

Redundancy analysis

Redundancy analysis (RDA) was employed to determine potential correlations between methylation variants and environmental variables, including altitude, oxygen partial pressure, and climatic factors such as minimum and maximum temperature and precipitation from 2000 to 2019 (Forester et al., 2018; Gugger et al., 2016; Williams et al., 2023). Methylation positions extracted from DMGs were analyzed in relation to these conditions. Data on altitude, minimum and maximum temperatures, and precipitation across the habitats of the two snub-nosed monkey species were acquired from WorldClim (https://www.worldclim.org/) with a spatial resolution of 5 min, while oxygen partial pressure was calculated using the Altitude Air Pressure Calculator (https://altitudecontrol.com/altitude-air-pressure-calculator/). Environmental variable selection was carried out using the "*vifstep*" function in the R package "usdm" to identify variables with a Variance Inflation Factor (VIF) lower than 10 (Naimi et al., 2014), ensuring the inclusion of the most important and least collinear variables. The selected environmental variables were then used in RDA using the "vegan" R package (Oksanen et al., 2022).

Gene enrichment analysis

DMGs with significant methylation differences were subjected to functional enrichment analysis using the R package clusterProfiler (Yu et al., 2012). Gene enrichment analysis was performed based on Gene Ontology (GO) biological process (BP) terms and Kyoto Encyclopedia of Genes and Genomes (KEGG) pathways. Terms and pathways with a *P*-value less than 0.05 were considered significantly enriched.

Functional validation of DMGs

Given the position-dependent regulatory effects of DNA methylation on gene expression and the association of methylation sites with the promoter regions of candidate genes *SNX10*, *TIMELESS*, and *CACYBP*, we investigated the functions of these three DMGs using expression assays to up-regulate and down-regulate their expression levels. The mRNA sequences of the relevant DMGs were downloaded from Ensembl (https://ensemblgenomes.org/) (*SNX10*: ENSRROT00000044888.1, *TIMELESS*: ENSRBIT00000013822.1, *CACYBP*: ENSRBIT00000058243.1). The coding sequences were synthesized and cloned into the pcDNA3.1-myc-HisA (+) vector to construct recombinant pcDNA3.1-DMGs plasmids at Shanghai Sangon Biotech (China). A-549 cells were cultured into 96 well-plates in a 5% CO_2 incubator at 37℃. The medium was changed every 2–3 days, and the cells were passaged upon reaching confluence. For transient overexpression of the DMGs, cells at 80% confluence were transfected with plasmids using Lipofectamine 3000 transfection reagent (Invitrogen, USA). Firstly, Lipofectamine™ 3000 reagent was diluted in Opti-MEM™ medium (two tubes) and mixed well. Secondly, a master mix of DNA was prepared by diluting DNA in Opti-MEM™ medium, then adding P3000™ reagent and mixing well. Thirdly, diluted DNA was added to each tube of diluted Lipofectamine™ 3000 reagent (1:1 ratio). Finally, the mixture was incubated for 10–15 min at room temperature. The DNA-lipid complex was added to the cells. After incubation for 24 h at 37 °C, the transfected cells were visualized and analyzed under a microscope before subsequent processing.

Small interfering RNAs (siRNAs) were synthesized to down-regulate the expression of the candidate genes. A-549 cells (30% confluence) were transfected with 50 nmol/L (final concentration) siRNAs targeting *SNX10*, *TIMELESS*, and *CACYBP*. Control experiments were carried out using nontargeting siRNA. The sequences of the *SNX10* siRNA oligonucleotides were 5'-GGACACAGTAGTGATGACAGCAGTT-3' (siSNX10-1) and 5'-TCAACATGAACAATCGCCAGCATGT-3' (siSNX10-2), *TIMELESS* siRNA oligonucleotides were 5'-AGAAGAGAAGGAAGAAGAATT-3' (siTIMLESS-1) and 5'-GCCUACAUGUGCUAGAGAUTT-3' (siTIMLESS-3), and *CACYBP* siRNA oligonucleotides were 5'-GCGGCUUCGUGAUGUUCUATT-3' (siCACYBP-1) and 5'-GCGAAGGGCUUAUGAACCUTT-3' (siCACYBP-3) (Hanbio, China).

To mimic the effects of hypoxia-induced DNA damage and endoplasmic reticulum (ER) stress in cells (Kimura-Ohba & Yang, 2016; Li et al., 2011), we used etoposide to induce DNA damage and thapsigargin and tunicamycin to induce ER stress. Additionally, we designed UV exposure experiments to simulate DNA damage induced by UV exposure (Palomera-Sanchez & Zurita, 2011). Twenty-four hours after transfection with pcDNA3.1-DMG plasmid tagged by EGFP and 48 h after transfection with siRNA, cells were treated with 20 μmol/L etoposide, 1 μmol/L thapsigargin, 2 μg/mL tunicamycin or left untreated for 24 h in 5% CO_2 incubator at 37 ºC, respectively. Each treatment was repeated six times. For the UV exposure experiments, cells were exposed in UV light for 15 s, 30 s, or 45 s, or left untreated, then cultured for 24 h in a 5% CO_2 incubator at 37 °C. DNA damage and ER stress were evaluated using a WST-1 cell viability assay, and cell mortality rates were calculated.

RESULTS

Conservation of genome-wide DNA methylation profiles in snub-nosed monkeys compared to other vertebrates

Approximately 5.6 billion reads were generated by WGBS from 15 samples of Yunnan and golden snub-nosed monkeys, averaging about 373 million reads per individual. Of these reads, approximately 72% were mapped to the golden snub-nosed monkey reference genome, and about 51% were mapped to distinct genomic regions (Supplementary Table S2). The global CpG methylation level in the snub-nosed monkey genome ranged from 69.3% to 79.0% (Supplementary Table S3), consistent with the methylation levels observed in other mammals (Al Adhami et al., 2022; Hon et al., 2013; Ziller et al., 2013). The global CG methylation (69.3%–79.0%) was markedly higher than CHG methylation (0.10%–0.40%) and CHH methylation (0.10%–0.50%). PCA revealed species-specific DNA methylation patterns between the two snub-nosed monkey species (Figure 1C), suggesting that environmental factors, rather than technical confounders, are likely responsible for

the observed differential methylation. The predominant feature of their methylation patterns —high overall genomic methylation with reduced methylation at gene transcription start sites (TSS) (Figure 1D, E) —mirrors findings in the methylomes of other vertebrates (Al Adhami et al., 2022).

Results indicated that most methylation peaks were distributed in introns, followed by exons, 2k bp region upstream of TSS, 3'-untranslated regions (UTRs), and 300 bp region downstream of transcription termination sites, with fewer peaks identified in 5'-UTRs (Figure 1F; Supplementary Table S4). There was a small but significant increase in overall DNA methylation levels in golden snub-nosed monkeys compared to Yunnan snub-nosed monkeys (P<0.05, Mann-Whitney U test), indicating that the Yunnan snub-nosed monkey genome was relatively more hypomethylated (Figure 1F, G). Previous studies have reported that extensive methylation of cancer cell chromatin is reduced under tumor hypoxic conditions, potentially influencing gene expression regulation and promoting tumor progression (Pal et al., 2010; Shahrzad et al., 2007). Given that Yunnan snub-nosed monkeys experience more severe hypoxic environments than golden snub-nosed monkeys, we hypothesize that the reduction in methylation in the Yunnan snub-nosed monkey genome may be a response to the more severe hypoxia they endure, leading to alterations in DNA methylation across most of their chromatin.

DMGs between Yunnan and golden snub-nosed monkeys

Comparison of the DNA methylation profiles between Yunnan and golden snub-nosed monkeys identified a total of 44 743 DMRs. The majority of these DMRs were located in intergenic regions (60%), followed by introns (30%), exons (6%), and promoter regions (3%) (Figure 2A). Among these, 23 142 DMRs exhibited higher methylation levels in golden snub-nosed monkeys compared to Yunnan snub-nosed monkeys and were thus classified as hypermethylated. Conversely, 21 601 DMRs displayed lower methylation levels in golden snub-nosed monkeys and were classified as hypomethylated. The hyper- and hypomethylation patterns were distinct in their distribution: hypermethylated DMRs were predominantly located in intergenic regions (69%), followed by introns (26%), exons (4%), and promoter regions (2%) (Figure 2B), while hypomethylated DMRs were primarily found in intergenic regions (59%), followed by introns (31%), promoter regions (5%), and exons (4%) (Figure 2C). RDA of methylation variants and environmental factors revealed that altitude, or indirectly oxygen partial pressure, had the most significant impact on methylation patterns (Figure 2D, E; Supplementary Figure S2A, B), further suggesting that the DMGs identified in our study are associated with the hypoxic conditions encountered in high-altitude habitats.

The hypermethylated genes identified in the golden snub-nosed monkeys were predominantly associated with membrane fusion and vesicle-related biological processes. In regions with significant methylation differences, we identified 160 genes potentially regulated by these DMRs (Figure 2F). Of these 160 DMGs, 58 exhibited increased methylation (hypermethylated) and 102 exhibited reduced methylation (hypomethylated) in the golden snub-nosed monkeys compared to the Yunnan snub-nosed monkeys. These DMGs were ranked based on the methylation differences of the corresponding DMPs/DMRs in descending order. The top 10 hypermethylated genes in the golden snub-nosed monkeys compared to the Yunnan snub-nosed monkeys were *SNX10*, *PLEKHG3*, *ZNF432*, *ARFGEF1*, *LRRC39*, *ADAM5*, *PMS1*, *DCSTAMP*, *ZNF343,* and *SLC13A3*. Conversely, the top 10 hypomethylated genes in the golden snub-nosed monkeys relative to the Yunnan snub-nosed monkeys were *TIMELESS*, *CACYBP*, *UPF3A*, *ZNF266*, *GNPAT*, *USP45*, *NMRK1*, *PRRC2C*, *CNTNAP1*, and *EIF4G2* (Figure 2F; Supplementary Table S5). The hypermethylated DMGs in golden snub-nosed monkeys were significantly enriched in bone resorption (P=1.7×10^{-3}, Fisher's exact test), organelle assembly (P=2.7×10^{-3}, Fisher's exact test), bone remodeling (P=3.6×10^{-3}, Fisher's exact test), organelle fusion (P=6.4×10^{-3}, Fisher's exact test), phagocytosis (P=0.02, Fisher's exact test), and vesicle organization (P=0.03, Fisher's exact test) (Figure 2G; Supplementary Table S6). In addition, several hypermethylated DMGs in the golden snub-nosed monkeys, including *PLEKHG3* (Ettelt et al., 2023), *ARFGEF1* (Zhao et al., 2002), *MARCHF8* (Gauvreau et al., 2009), *RAC1* (Nakaya et al., 2008), *SFT2D3* (Liu et al., 2020), *RAB5A* (Hoffenberg et al., 2000), and *FYCO1* (Pankiv et al., 2010), were associated with vesicular trafficking, lysosomal function, membrane fusion, and regulation of apoptotic cell phagocytosis (Figure 3A; Supplementary Table S7). Moreover, *HBD* and *CLASP1* were found to be hypermethylated in golden snub-nosed monkeys and hypomethylated in Yunnan snub-nosed monkeys. These genes are important for obtaining adequate oxygen, with their up-regulation crucial under hypoxic conditions (An et al., 2022; De Souza Iung et al., 2018) (Figure 3A). Furthermore, *MET* and *CD36*, which are related to angiogenesis (Febbraio et al., 2001; You & McDonald, 2008), were also hypermethylated in golden snub-nosed monkeys and hypomethylated in Yunnan snub-nosed monkeys (Figure 3A).

The hypomethylated genes in golden snub-nosed monkeys were primarily involved in cell proliferation and differentiation. Notably, the hypomethylated DMGs in golden snub-nosed monkeys (hypermethylated in Yunnan snub-nosed monkeys) were significantly enriched in biological processes associated with sensory organ development and neuronal development and differentiation (*TDP2*, *OTP*, *B2M*, *PHACTR1*, *MARK1*, *IFT27*, and *VSX1*), including neuronal differentiation (P=3.7×10^{-3}, Fisher's exact test), sensory organ development (P=4.5×10^{-3}, Fisher's exact test), and the Wnt signaling pathway (P=9.7×10^{-3}, Fisher's exact test) (Figure 2E; Supplementary Table S5). The hypermethylated genes in the Yunnan snub-nosed monkeys, including *TIMELESS* (Somyajit et al., 2017), *USP45* (Griffis et al., 2007), *DHX36* (Zeng et al., 2020), *NABP1* (Huang et al., 2009), *MMS22L* (O'Donnell et al., 2010), *BUB3* (Logarinho et al., 2008), and *BARD1* (Schüchner et al., 2005), were involved in cell cycle processes, indicating that cell proliferation, especially in sensory functions, may be comparatively suppressed in Yunnan snub-nosed monkeys (Figure 3A; Supplementary Table S6). Genes involved in the Wnt signaling pathway, including *PRKACB*, *CACYBP*, *PRKCA*, and *FRZB*, were also hypermethylated in Yunnan snub-nosed monkeys (Figure 2E; Figure 3A; Supplementary Table S5), as were *TRPC6* and *TRDN* (Figure 3A). *TRPC6* is a non-selective calcium channel gene (Liao et al., 2008), while *TRDN* is an essential component of the macromolecular complex with another important Ca^{2+} channel, RyR1 (Goonasekera et al., 2007).

Comparison of known genes related to high-altitude adaptation with DMGs in snub-nosed monkeys

High-altitude adaptation has long been a focal point of interest

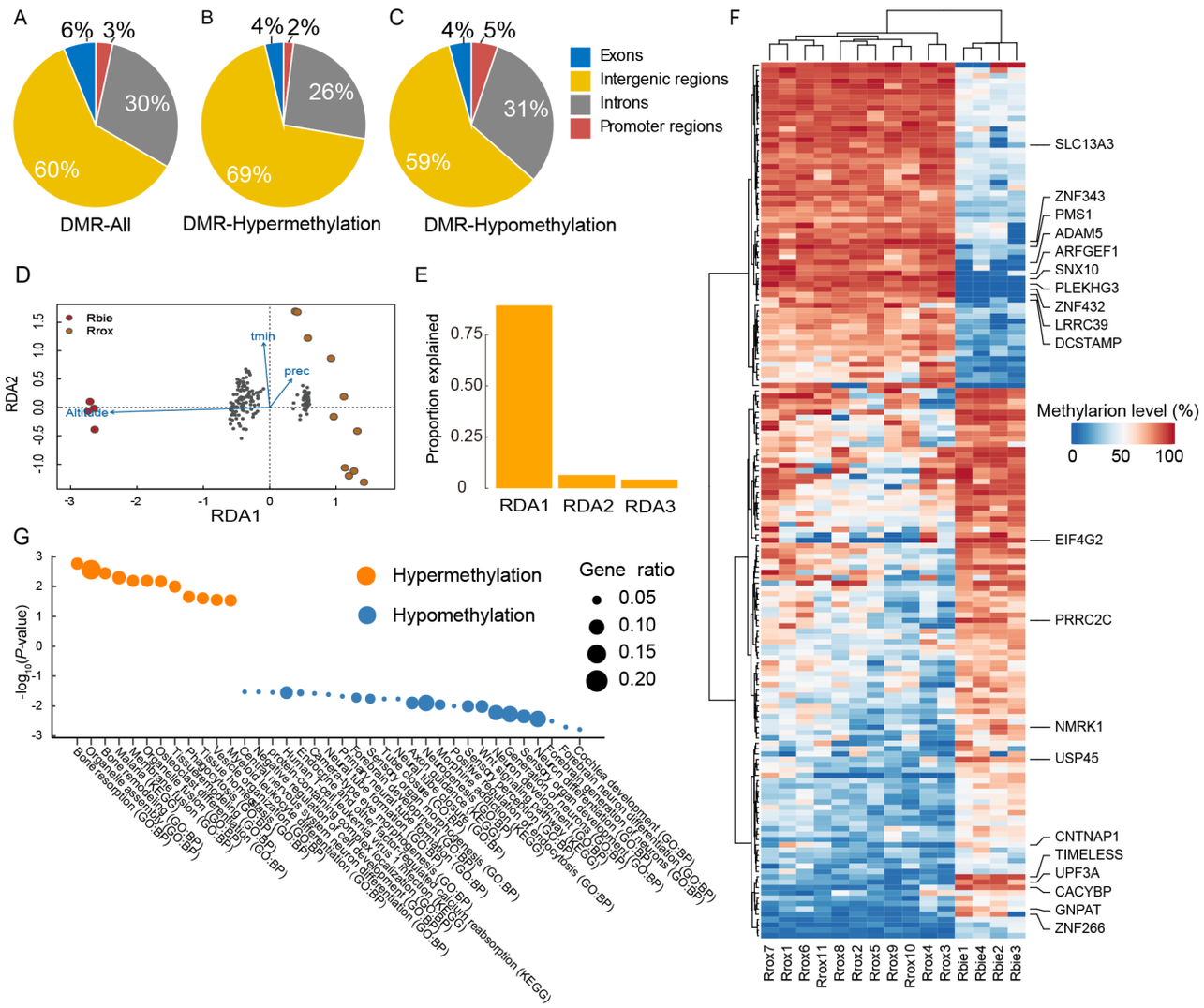

Figure 2 Comparative analysis of differentially methylated regions (DMRs) between golden and Yunnan snub-nosed monkeys, RDA of methylation variants in promoter regions and environmental factors, and DMG pathway enrichment analysis

A: Pie plot showing proportions of all DMRs (DMR-All) in exons, intergenic regions, introns, and promoter regions. B: Pie plot showing proportions of hypermethylated DMRs (DMR-Hypermethylation) in exons, intergenic regions, introns, and promoter regions in golden snub-nosed monkeys compared to Yunnan snub-nosed monkeys. C: Pie plot showing proportions of hypomethylated DMRs (DMR-Hypomethylation) in exons, intergenic regions, introns, and promoter regions in golden snub-nosed monkeys compared to Yunnan snub-nosed monkeys. D: PCA plot based on RDA axes 1 and 2. Blue arrows represent environmental variables. tmin: annual average minimum temperature, prec: annual total precipitation. Red and orange points represent Yunnan snub-nosed monkeys (Rbie) and golden snub-nosed monkeys (Rrox), respectively. Gray points represent differential methylation values of each position. E: Variance explained by RDA axes. F: Heatmap of all differentially methylated genes (DMGs). Top 10 hypermethylated and hypomethylated genes (golden snub-nosed monkeys compared to Yunnan snub-nosed monkeys) with methylation difference values. Color range represents hypomethylation (blue) to hypermethylation (red), Rrox: *Rhinopithecus roxellana*, Rbie: *R. bieti*. G: Gene enrichment based on GO (biological processes, BP) and KEGG analyses. X-axis represents pathway terms and Y-axis represents $-\log_{10}$(*P*-value). Point size represents gene ratio. Color represents hypermethylation (orange) and hypomethylation pathways (blue) in golden snub-nosed monkeys compared to Yunnan snub-nosed monkeys.

in humans and other mammals (Julian & Moore, 2019). Hundreds of genes associated with natural selection have been identified in the genomes of humans and mammals inhabiting elevated environments (Supplementary Table S7). For example, common genetic traits in HIF pathway genes have been observed in human populations from Xizang, the Andes, and Ethiopia (Bigham, 2016). Specifically, the *EGLN1* gene, which influences HIF-1α hydroxylation, shows signs of natural selection within these groups (Lorenzo et al., 2014; Simonson et al., 2010). Additionally, the *EPAS1* gene, associated with low hemoglobin levels in Xizang populations, has undergone significant natural selection (Beall et al., 2010). The adaptive significance of *EPAS1* is also evident in other mammals, such as North American deer mice (*Peromyscus maniculatus*), Andean horses (*Equus caballus*), and Xizang breeds of dogs (*Canis lupus familiaris*), goats (*Capra hircus*), horses (*Equus caballus*), and pigs (*Sus scrofa*), while natural selection in *EGLN1* has been observed in cattle (*Bos taurus*) (reviewed in Lee, 2024). Investigating the methylation patterns of HIF pathway genes under natural selection in humans (75 genes) and those associated with the GO “Response to Hypoxia” category (120 genes) (Ashburner et al., 2000;

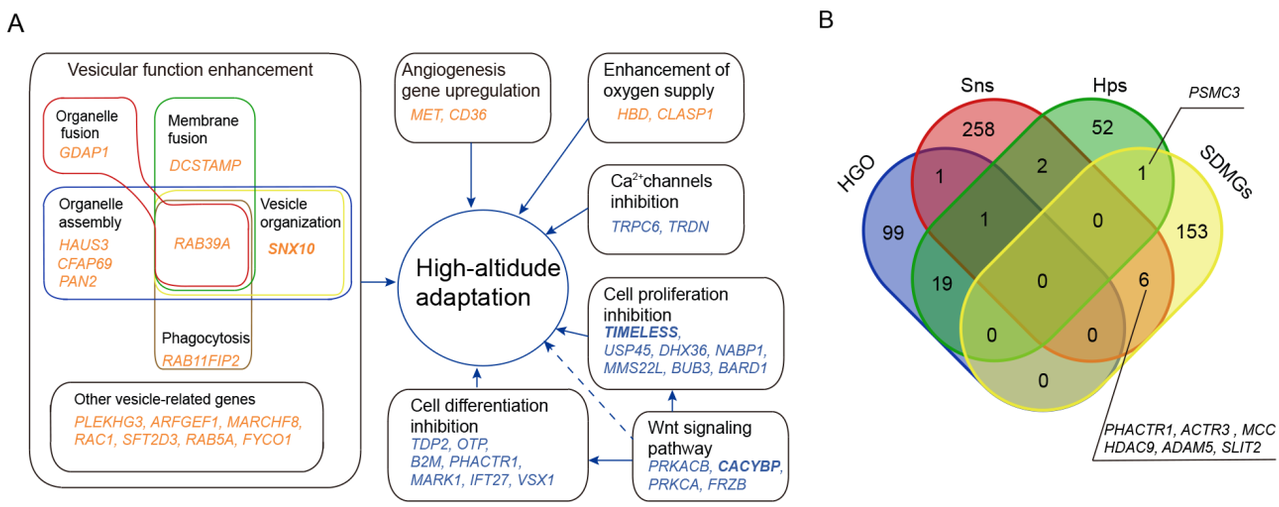

Figure 3 Potential epigenetic adaptations of DMGs in snub-nosed monkeys and comparative analyses of known hypoxia adaptation genes

A: DMGs involved in hypoxic adaptation. Golden snub-nosed monkey hypermethylated DMGs (compared to Yunnan snub-nosed monkeys) are shown in orange and hypomethylated DMGs are shown in blue. Genes in bold are the three selected for further functional validation. B: Venn diagram showing overlapping genes among human positive selection genes, GO "Response to Hypoxia" genes, snub-nosed monkey natural selection genes, and DMGs identified in our study. HGO: Human candidate genes in GO "Response to Hypoxia" with experimental evidence, Sns: Snub-nosed monkey natural selection genes, Hps: Human positive selection genes, SDMGs: Snub-nosed monkey DMGs in our study. Overlapping genes are labeled in the figure.

Carbon et al., 2009) ("2023-11-17" and "DOI: 10.5281/zenodo.10162580") could provide further insights. Nevertheless, among these recognized genes, only *PSMC3* showed hypermethylation in the Yunnan snub-nosed monkeys compared to the golden snub-nosed monkeys (Figure 3B). *PSMC3* encodes the 26S proteasome regulatory subunit 6A, a component of the proteasome complex that can inhibit Hif1-α through interaction with p14ARF (Corn et al., 2003; Pollice et al., 2008). Therefore, the hypermethylation of *PSMC3* may repress its function, potentially representing an adaptive feature that enhances cellular resistance to hypoxia in Yunnan snub-nosed monkeys.

We compared the DMGs identified in our study with genes implicated in high-altitude adaptation across animal species. Notably, *TIMELESS*, the primary hypomethylated DMG in golden snub-nosed monkeys compared to Yunnan snub-nosed monkeys, also exhibits positive selection in geladas (*Theropithecus gelada*) (Chiou et al., 2022). *PLA2G12A*, *SYNE1*, and *NBEAL1* have also been identified in high-altitude rhesus macaques (*Macaca mulatta*) based on haplotype-based scans (Szpiech et al., 2021), while the hypomethylated DMG *PLXNA4* is implicated in high-altitude adaptation in the Himalayan Mountain dog (*Canis lupus familiaris*) (Li et al., 2014). *FOXN2*, hypermethylated in golden snub-nosed monkeys relative to Yunnan snub-nosed monkeys, shows positive selection in cashmere goats inhabiting Xizang (Song et al., 2016), with *ATP8B4* and *FOXN2* similarly under positive selection in Xizang sheep (*Ovis aries*) (Wei et al., 2016). Despite these correlations, our results showed a lack of significant overlap between the identified DMGs and genes exhibiting selection signatures in other species, suggesting that the convergence of genetic and epigenetic factors for high-altitude adaptation may not be straightforward or common across different species.

Based on population genomics, previous studies have identified 268 genes under natural selection in Yunnan snub-nosed monkeys (Yu et al., 2016; Zhou et al., 2014). Among these genes, our results showed that *PHACTR1*, *ACTR3*, and *MCC* were hypermethylated, while *HDAC9*, *ADAM5*, and *SLIT2* were hypomethylated in Yunnan snub-nosed monkeys (Figure 3B). Several of these genes are potentially connected to high-altitude adaptation. For instance, *PHACTR1*, associated with vascular development and endothelial cell survival, is regulated by *VEGFA*, a gene within the HIF pathway (Allain et al., 2012; Jarray et al., 2011). Despite these findings, limited overlap was observed among the genes undergoing natural selection in Yunnan snub-nosed monkeys and those with altered methylation (Figure 3B), suggesting different dimensions of adaptation through evolution. The HIF pathway and its downstream genes are involved in many processes (Bigham & Lee, 2014), including cell cycle control (Semenza, 2011), cell proliferation and differentiation (Hubbi & Semenza, 2015), energy metabolism (Das, 2006; Hermes-Lima et al., 2015; Prentki & Madiraju, 2008), angiogenesis (Pugh & Ratcliffe, 2003), and immune response (Nizet & Johnson, 2009). Although most identified DMGs were not found on the list of known HIF pathway genes, they may still be associated with these genes and play an important role in hypoxic adaptation. However, the specific functions of these DMGs in relation to hypoxic adaptation need further verification.

Expression levels of DMGs in snub-nosed monkeys influence cell survival in stressful environments

Differential methylation analysis between golden and Yunnan snub-nosed monkeys identified *SNX10* as the top hypermethylated DMG (methylation difference value=92.14%, P=6.76×10^{-115}). The top two hypomethylated DMGs in golden snub-nosed monkeys were *TIMELESS* (methylation difference value=–70.16%, P=2.29×10^{-62}) and *CACYBP* (methylation difference value=–67.12%, P=2.39×10^{-119}) (Figure 3A; Supplementary Table S5). To investigate the role of methylation in these genes regarding high-altitude adaptation, expression assays were conducted under various stress

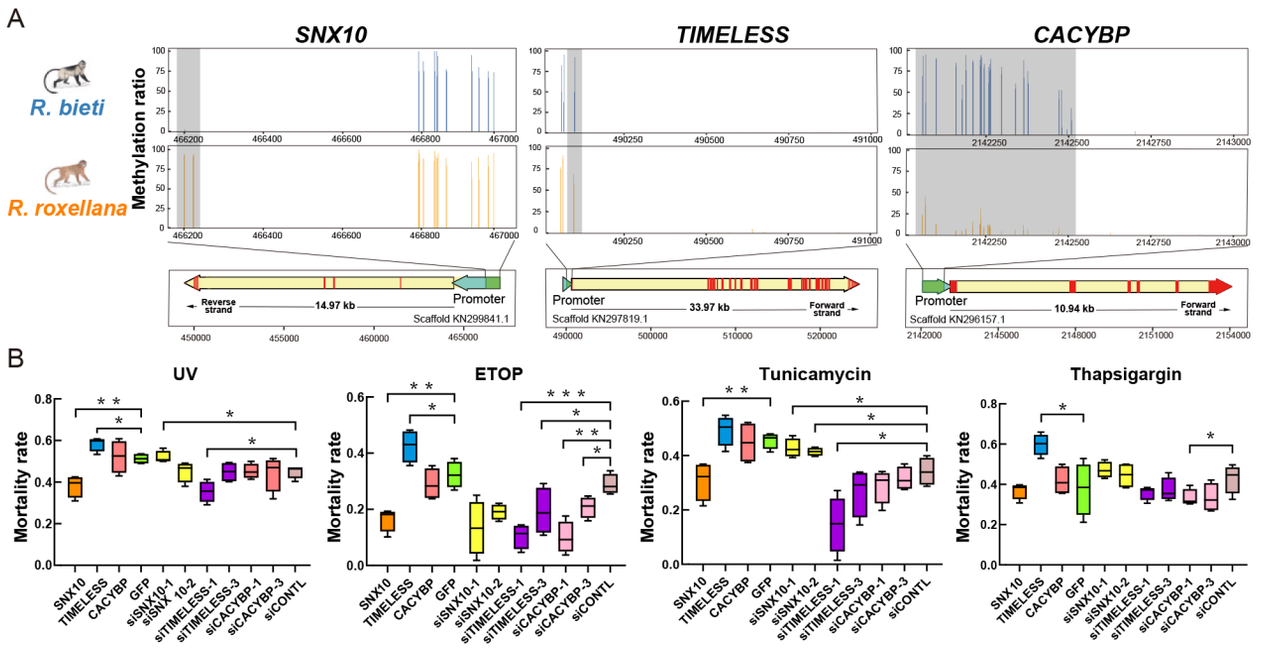

Figure 4 Structure of DMGs and cellular assay under various stress conditions

A: Representative images of methylation levels for DMGs related to high-altitude adaptation. B: Mortality rate assay of cells with pcDNA3.1-DMG plasmids tagged by EGFP treated under stress conditions and mortality rate assay of siRNAs targeting *SNX10*, *TIMELESS*, and *CACYBP* treated under stress conditions, UV: Cells in UV exposure experiment, ETOP: Cells treated with etoposide, Tunicamycin: cells treated with tunicamycin, Thapsigargin: Cells treated with thapsigargin, asterisks indicating statistical significance in *t*-test are marked in B, *: $P<0.05$; **: $P<0.01$; ***: $P<0.001$.

conditions (Figure 4A, B; Supplementary Figure S3). Cells overexpressing *SNX10* from snub-nosed monkeys demonstrated significantly lower mortality rates than controls under UV exposure and DNA damage induced by etoposide ($P<0.01$, *t*-test) (Figure 4B). Similarly, cells overexpressing *SNX10* showed lower mortality rates than controls under ER stress induced by tunicamycin ($P<0.01$, *t*-test) (Figure 4B). Conversely, cells with *SNX10* knockdown via siRNA showed significantly higher mortality rates in UV and tunicamycin-induced ER stress tests ($P<0.05$, *t*-test) (Figure 4B), further emphasizing the potential protective role of *SNX10*. These results suggest that elevated SNX10 levels may enhance cell survival under stress, while reduced *SNX10* expression may impair it.

The experimental group overexpressing *TIMELESS* exhibited a higher cell mortality rate than the control group under UV exposure, DNA damage induced by etoposide, and ER stress induced by thapsigargin ($P<0.05$, *t*-test) (Figure 4B). Conversely, the experimental group with *TIMELESS* knockdown via siRNA exhibited a significantly lower cell mortality rate than the control group under UV exposure ($P<0.05$, *t*-test), DNA damage induced by etoposide ($P<0.01$, *t*-test), and ER stress induced by tunicamycin ($P<0.05$, *t*-test). These findings indicate that *TIMELESS* overexpression may decrease cell survivability under stress, while *TIMELESS* knockdown may improve it (Figure 4B).

In the experiments involving UV exposure, DNA damage with etoposide, and ER stress with tunicamycin and thapsigargin, cells overexpressing *CACYBP* did not show significant changes in mortality compared to the control group (Figure 4B). However, cells with reduced *CACYBP* expression exhibited a significant decrease in mortality in the DNA damage and ER stress experiments ($P<0.05$, *t*-test), indicating that *CACYBP* knockdown may enhance cell survival under stress.

DISCUSSION

Gene regulation through DNA methylation is potentially beneficial to high-altitude adaptation

Our study identified significant differences in methylation patterns within the promoter regions of DMGs. Promoter methylation can influence gene expression by affecting transcription factor binding, recruiting methyl-CpG binding proteins that alter chromatin architecture (Bommarito & Fry, 2019; Boyes & Bird, 1991; Du et al., 2015; Watt & Molloy, 1988), or modulating the expression of specific genes, especially transcription factors (Moarii et al., 2015), ultimately regulating gene function. Based on these findings, we hypothesize that the notable methylation differences identified in our analysis may exert distinct effects on the functional performance of DMGs in golden snub-nosed monkeys compared to Yunnan snub-nosed monkeys.

The hypomethylation of vesicular-related genes found in Yunnan snub-nosed monkeys suggests a significant adaptation to low oxygen conditions. Under hypoxic stress, cells undergo protein modifications and accumulate unfolded and misfolded proteins. These proteins are then degraded through ER-associated degradation and autophagy, which help mitigate ER stress and preserve cell function (Hetz, 2012). Chronic hypoxia induces the autophagic removal of damaged macromolecules and organelles, recycling nutrients and promoting cell survival, a process often observed in hypoxic areas of solid tumors (Rouschop et al., 2010). Damaged or dead cells due to hypoxia are eliminated through phagocytosis, a mechanism associated with membrane fusion and vesicles (Pizzo & Pozzan, 2007; Rosales & Uribe-Querol, 2017; Wang & Klionsky, 2003). Hypermethylated DMGs in golden snub-nosed monkeys were enriched in “organelle assembly” (*RAB39A*, *HAUS3*, *SNX10*, *CFAP69* and *PAN2*), “membrane fusion” (*RAB39A* and *DCSTAMP*), “organelle

fusion" (*GDAP1* and *RAB39A*), "phagocytosis" (*RAB39A* and *RAB11FIP2*), and "vesicle organization" (*RAB39A* and *SNX10*) (Figure 2E; Figure 3A; Supplementary Table S6). These genes, hypermethylated in the promoter proximal regions in golden snub-nosed monkeys and hypomethylated in Yunnan snub-nosed monkeys, may lead to an enhanced functional response in Yunnan snub-nosed monkeys, potentially associated with adaptations to the hypoxic conditions of high-altitude environments. For instance, *RAB39A*, a member of the RAS oncogene family, is connected to vesicle trafficking (Gambarte Tudela et al., 2015) and has been shown to increase under hypoxic conditions in various cancer cell types (Chano et al., 2018). Other hypermethylated DMGs in golden snub-nosed monkeys, such as *PLEKHG3* (Ettelt et al., 2023), *ARFGEF1* (Zhao et al., 2002), *MARCHF8* (Gauvreau et al., 2009), *RAC1* (Nakaya et al., 2008), *SFT2D3* (Liu et al., 2020), *RAB5A* (Hoffenberg et al., 2000), and *FYCO1* (Pankiv et al., 2010), are also implicated in vesicular trafficking, lysosomal function, membrane fusion, and regulation of phagocytosis of apoptotic cells. RAC1, a GTPase protein of the RAS superfamily, activates and binds to various effector proteins, affecting cellular processes including phagocytosis, migration, differentiation, and membrane ruffle formation (Nakaya et al., 2008; Ridley et al., 1992; Zhao et al., 2013). Hypoxia can also up-regulate RAC1 mRNA levels and activity over time (Xue et al., 2006). In summary, membrane fusion and vesicles play critical roles in the cellular response to hypoxia, with hypoxia altering the number and contents of secreted vesicles (Chen et al., 2018; Walbrecq et al., 2020).

Hypoxia-inducible factor 1α (HIF1A), as a master regulator of the cellular response to hypoxia, is continuously synthesized and degraded by the ubiquitin-proteasome system under normoxic conditions, but accumulates rapidly under hypoxia (Salceda & Caro, 1997). It induces the transcription of hundreds of genes involved in hypoxia adaptation (Akman et al., 2021; Semenza, 2012). Hence, preventing the degradation of HIF1A is critical for the cellular response to hypoxia. In this study, *PAN2* was identified as a hypomethylated DMG in Yunnan snub-nosed monkeys, suggesting enhanced functional activity or expression relative to its counterpart in the golden snub-nosed monkeys (Figure 3A). PAN2 acts as a regulator of HIF1A mRNA stability, and its reduction decreases HIF1A mRNA and protein levels (Bett et al., 2013). Similarly, *HBD*, which encodes the hemoglobin subunit delta responsible for transporting oxygen from the lungs to peripheral tissues (Moleirinho et al., 2015), was also hypomethylated in Yunnan snub-nosed monkeys. This hypomethylation implies an enhanced function of *HBD*, potentially aiding in oxygen extraction under hypoxic conditions, as observed in plateau pika (*Ochotona curzoniae*), with the specific up-regulation of *HBD* in lung tissues considered crucial for survival in high-altitude, hypoxic environments (An et al., 2022). In addition, *CLASP1*, another hypomethylated DMG in Yunnan snub-nosed monkeys, is involved in the regulation of blood pressure (De Souza lung et al., 2018). The hypomethylation of *CLASP1* suggests enhanced function (Figure 3A), potentially aiding in the regulation of blood pressure to ensure adequate oxygen supply.

Hypermethylated DMGs in Yunnan snub-nosed monkeys, such as *TDP2*, *OTP*, *B2M*, *PHACTR1*, *MARK1*, *IFT27*, and *VSX1*, were significantly enriched in biological processes associated with neuronal development and differentiation (Figures 2E, 3A; Supplementary Table S5). This finding aligns with previous research on the Chinese grouse (*Tetrastes sewerzowi*), which reported GO enrichment in nervous system development or death as an adaptation to hypobaric hypoxia and high UV radiation in high-altitude habitats (Song et al., 2022). Neurons are particularly sensitive to oxygen deprivation, and hypoxia is known to impede cell differentiation (Felfly et al., 2011; Majmundar et al., 2015). Notably, the hypermethylation of DMGs in Yunnan snub-nosed monkeys suggests a suppression of genes related to neuronal differentiation (Figure 2E). Furthermore, other identified hypermethylated genes, including *TIMELESS* (Somyajit et al., 2017), *USP45* (Griffis et al., 2007), *DHX36* (Zeng et al., 2020), *NABP1* (Huang et al., 2009), *MMS22L* (O'Donnell et al., 2010), *BUB3* (Logarinho et al., 2008), and *BARD1* (Schüchner et al., 2005), play roles in the cell cycle, suggesting that cell proliferation, particularly in sensory functions, may be comparatively inhibited in Yunnan snub-nosed monkeys (Figure 3A; Supplementary Table S6). As cell proliferation increases demand for oxygen and aggravates hypoxic stress, hypoxia generally inhibits cell proliferation (Hubbi & Semenza, 2015). This inhibition of cell proliferation may be an adaptive measure for Yunnan snub-nosed monkeys. Furthermore, several hypermethylated DMGs in Yunnan snub-nosed monkeys were enriched in the Wnt signaling pathway (*PRKACB*, *CACYBP*, *PRKCA*, and *FRZB*) (Figure 3A; Supplementary Table S5). Hypoxia has been reported to negatively regulate skeletal myogenesis through the inhibition of canonical Wnt signaling during adult muscle regeneration (Majmundar et al., 2015). Accordingly, hypoxic adaptation in Yunnan snub-nosed monkeys may involve the inhibition of cell proliferation and differentiation, potentially via inhibition of the Wnt signaling pathway.

TRPC6, hypermethylated in the Yunnan snub-nosed monkey, encodes a non-selective calcium channel that is crucial for various cellular functions, including gene transcription, cell proliferation, and apoptosis (Liao et al., 2008; Wang & Zheng, 2010). Research has shown that in the absence of dystrophin, *TRPC6* deletion reduces cell damage in mice (Lin et al., 2022). Additionally, knockdown of *TRPC6* prevents apoptosis of renal tubular epithelial cells under oxidative stress (Hou et al., 2018), possibly by reducing Ca^{2+} overload via the PI3K/AKT and ERK pathways (Hou et al., 2021). Under hypoxic conditions, increased mitochondrial reactive oxygen species (ROS) can directly cause extracellular Ca^{2+} influx by opening store-operated Ca^{2+} (SOC) channels (Wang & Zheng, 2010). Therefore, regulating TRPC6 activity may help mitigate such damage, suggesting that its hypermethylation in Yunnan snub-nosed monkeys likely represents an adaptation to low-oxygen conditions (Figure 3A).

Another critical Ca^{2+} channel is the ryanodine receptor (RyR) Ca^{2+} release channel, essential for striated muscle contraction and contributing to diverse neuronal functions, including synaptic plasticity (Hidalgo et al., 2005). Through Ca^{2+}-induced Ca^{2+}-release (CICR), RyRs amplify and propagate initial Ca^{2+} signals triggered by Ca^{2+} entry, thereby regulating Ca-dependent pathways linked to specific cellular responses. In this study, *TRDN*, the gene encoding triadin, was found to be hypermethylated in Yunnan snub-nosed monkeys. Triadin, along with junctin, is an essential component of the macromolecular complex with RyR1,

facilitating rapid Ca^{2+} release (Goonasekera et al., 2007) and depolarization-induced Ca^{2+} release in skeletal muscle (Wang et al., 2009). The hypermethylation of *TRDN* could lead to a down-regulation of its function, potentially inhibiting RyR channels and reducing the harmful effects of excessive RyR-mediated CICR stimulation under hypoxic conditions (Figure 3A).

Functional inference of DMGs from expression assays

The *SNX10* gene was found to be hypomethylated in promoter-associated regions of Yunnan snub-nosed monkeys, indicating a potential up-regulation of its function compared to golden snub-nosed monkeys. This was corroborated by cellular assays, which demonstrated that increased *SNX10* expression enhanced cell survival under stressful conditions, whereas its suppression compromised cellular resilience (Figure 4B). SNX10, a member of the sorting nexin family, plays a critical role in vesicular trafficking and cellular homeostasis (Chen et al., 2012; Huybrechts & Van Hul, 2022). Overexpression of exogenous *SNX10* in cells leads to the formation of giant vacuoles (Qin et al., 2006), while its knockdown promotes cell growth and enhances glucose metabolism by triggering the mTORC1 pathway (Feng et al., 2023). *SNX10* is also involved in regulating endosome/lysosome homeostasis, acting as an adaptor protein to mediate signaling transduction and intracellular protein trafficking (Bao et al., 2023; Sultana et al., 2020; Wang et al., 2021). In this context, we propose that *SNX10* overexpression could be advantageous for organelle formation and vesicle function, promoting cellular resilience during stress, including hypoxia. Conversely, a reduction in SNX10 may disrupt membrane stability and adversely affect cell survival.

Cellular assays indicated that overexpression of *TIMELESS* reduced cell survival under stress, while silencing *TIMELESS* appeared to improve it (Figure 4B). *TIMELESS* encodes the highly conserved protein TIMELESS (Timeless Circadian Regulator, or TIM), which plays an important role in S phase checkpoint responses, replication fork progression (Cho et al., 2013), maintenance of telomere length and integrity (Leman et al., 2012), DNA repair, genome stability (Somyajit et al., 2017; Xie et al., 2015), and regulation of the circadian clock (Kurien et al., 2019). In the absence of TIMELESS or its displacement from the replication apparatus, such as in U2OS cells, replication fork progression is hindered (Somyajit et al., 2017; Ünsal-Kaçmaz et al., 2007). Our analysis revealed that the promoter region of *TIMELESS* was hypermethylated in Yunnan snub-nosed monkeys, potentially resulting in its functional suppression compared to golden snub-nosed monkeys. Considering the higher altitudes and increased UV exposure experienced by Yunnan snub-nosed monkeys, we suggest that the suppression of *TIMELESS* function through methylation may be an adaptive mechanism to manage stress more effectively.

Based on our cellular assays, *CACYBP* knockdown appeared to enhance cell survival under stress (Figure 4B). CACYBP is a versatile protein implicated in protein de-phosphorylation and ubiquitination, cytoskeletal dynamics, and gene regulation, affecting cell growth, differentiation, and cancer development (Topolska-Woś et al., 2016). Its exact role in proliferation and cancer is not fully understood, but it has been linked to abnormal β-catenin levels, a hallmark of many cancers, and the CACYBP target, S100A6 (Topolska-Woś et al., 2016). In Saos-2 cells, reduced CACYBP hinders cell growth, causing G1/S phase arrest, a decrease in cyclin-dependent kinase (CDK) and cyclin levels, and an increase in inhibitory protein p21 (Zhao et al., 2020). CDKs are crucial for cell cycle regulation (Malumbres 2014), while p21 plays a key role in cell cycle control and DNA damage response (LaBaer et al., 1997). The hypermethylation of *CACYBP* in Yunnan snub-nosed monkeys and its involvement in Wnt/β-catenin signaling may facilitate cell survival via this pathway, potentially influencing cellular outcomes in high-altitude environments.

Implications and limitations of this study

Molecular chronology suggests that snub-nosed monkeys, especially the golden and Yunnan species, underwent a rapid evolutionary expansion within the last 1.60 million years (Zhou et al., 2014). However, our genome-wide methylation analysis revealed a significant epigenetic divergence between these species, pointing towards an accumulation of epigenetic variations, potentially facilitated by rapid adaptive processes. Additionally, through differential methylation analysis and functional assays, we identified specific regions and genes contributing to local adaptations. These findings suggest that conservation strategies for these threatened primates should include epigenetic data to complement insights from traditional evolutionary history and genetic diversity.

Despite the strengths of our study, several limitations warrant consideration. First, the small and uneven sample sizes may have affected our results. Given that the Yunnan and golden snub-nosed monkeys are among the world's rarest primates, obtaining larger sample sizes is challenging. While we employed a semi-randomized sampling technique to achieve balanced representation across our comparative analyses and minimize the effects of uneven sample sizes, this approach did not entirely eliminate the potential for bias introduced by limited sample sizes. Second, various factors known to influence DNA methylation, such as age (Salameh et al., 2020; Zaghlool et al., 2015), sex (Govender et al., 2022), diet (Elgendy et al., 2018; Heijmans et al., 2008; Hibler et al., 2019; Mehta et al., 2017), social status, and behavior (Hilliard et al., 2019; Lenkov et al., 2015), were not incorporated into our comparative methylation analysis. Future studies should assess the impact of these factors on DNA methylation and develop refined methods to quantify their effects more precisely. Third, our analysis lacked mRNA data for the DMGs due to the suboptimal quality of samples, which were difficult to collect post-mortem and spread over an extensive timeframe. Consequently, we focused our discussion on DMGs with methylation alterations in the promoter regions. If mRNA and/or other related data had been available, it would have allowed a deeper understanding of the functions of these DMGs. Future research should aim to include high-quality mRNA data to provide more comprehensive insights.

CONCLUSIONS

Using WGBS, we obtained high-resolution, comprehensive DNA methylation profiles of golden and Yunnan snub-nosed monkeys. This study demonstrated that comparative genomic methylation analysis of closely related species can provide valuable insights into environmental adaptation mechanisms. The DMGs identified in this study may accelerate the discovery of critical genes involved in high-altitude adaptation, ultimately elucidating the underlying mechanisms. Our cellular

assays also indicated that varying expression levels of the candidate genes induced different phenotypes, suggesting that the genes associated with high-altitude tolerance may also broaden our understanding of altitude sickness and hypoxia-related conditions. These insights are not limited to the genes themselves but also consider their different methylation states, which may directly or indirectly affect gene function repression or enhancement. Future conservation strategies for these at-risk groups should integrate epigenetic information alongside conventional focus areas such as evolutionary history and genetic variability. However, the discrepancy between functional outcomes observed in cellular experiments and actual environmental adaptation cannot be disregarded. These preliminary findings necessitate further investigation through more extensive sampling and the use of precise experimental models.

DATA AVAILABILITY

The whole-genome bisulfite sequencing data obtained in this study were deposited in the Science Data Bank (https://www.scidb.cn/) under DOI: 10.57760/sciencedb.14868, Genome Sequence Archive (Genomics, Proteomics & Bioinformatics 2021) in National Genomics Data Center (Nucleic Acids Res 2022), China National Center for Bioinformation / Beijing Institute of Genomics, Chinese Academy of Sciences (GSA: CRA016400) that are publicly accessible at https://ngdc.cncb.ac.cn/gsa (Chen et al., 2021; CNCB-NGDC members & partners, 2021), and NCBI under BioProjectID PRJNA1144163.

SUPPLEMENTARY DATA

Supplementary data to this article can be found online.

COMPETING INTERESTS

The authors declare that they have no competing interests.

AUTHORS' CONTRIBUTIONS

Ming L. conceived and supervised the project. L.W. and W.Q.L. prepared the samples and performed bioinformatic analyses. R.F.W. helped with the bioinformatic analyses. L.W., J.D., and Meng L. preformed the experiments. L.W. wrote the manuscript with input from all authors. All authors read and approved the final version of the manuscript.

ACKNOWLEDGMENTS

We thank Dr. Xu-Ming Zhou from the Institute of Zoology, Chinese Academy of Sciences, for comments on an earlier draft of this manuscript. We also thank the anonymous reviewers for their helpful comments.

REFERENCES

Akalin A, Kormaksson M, Li S, et al. 2012. methylKit: a comprehensive R package for the analysis of genome–wide DNA methylation profiles. *Genome Biology*, **13**(10): R87.

Akman M, Belisario DC, Salaroglio IC, et al. 2021. Hypoxia, endoplasmic reticulum stress and chemoresistance: dangerous liaisons. *Journal of Experimental & Clinical Cancer Research*, **40**(1): 28.

Al Adhami H, Bardet AF, Dumas M, et al. 2022. A comparative methylome analysis reveals conservation and divergence of DNA methylation patterns and functions in vertebrates. *BMC Biology*, **20**(1): 70.

Allain B, Jarray R, Borriello L, et al. 2012. Neuropilin-1 regulates a new VEGF-induced gene, *Phactr*-1, which controls tubulogenesis and modulates lamellipodial dynamics in human endothelial cells. *Cellular Signalling*, **24**(1): 214–223.

An ZF, Wei LN, Xu B, et al. 2022. A homotetrameric hemoglobin expressed in alveolar epithelial cells increases blood oxygenation in high-altitude plateau pika (*Ochotona curzoniae*). *Cell Reports*, **41**(1): 111446.

Ashburner M, Ball CA, Blake JA, et al. 2000. Gene ontology: tool for the unification of biology. *Nature Genetics*, **25**(1): 25–29.

Ball MP, Li JB, Gao Y, et al. 2009. Targeted and genome-scale strategies reveal gene-body methylation signatures in human cells. *Nature Biotechnology*, **27**(4): 361–368.

Bao WL, You Y, Ni JH, et al. 2023. Inhibiting sorting nexin 10 promotes mucosal healing through SREBP2-mediated stemness restoration of intestinal stem cells. *Science Advances*, **9**(35): eadh5016.

Beall CM, Cavalleri GL, Deng LB, et al. 2010. Natural selection on *EPAS1* (*HIF2α*) associated with low hemoglobin concentration in Tibetan highlanders. *Proceedings of the National Academy of Sciences of the United States of America*, **107**(25): 11459–11464.

Bett JS, Ibrahim AFM, Garg AK, et al. 2013. The P-body component USP52/PAN2 is a novel regulator of *HIF1A* mRNA stability. *Biochemical Journal*, **451**(2): 185–194.

Bigham AW, Lee FS. 2014. Human high-altitude adaptation: forward genetics meets the HIF pathway. *Genes & Development*, **28**(20): 2189–2204.

Bigham AW. 2016. Genetics of human origin and evolution: high-altitude adaptations. *Current Opinion in Genetics & Development*, **41**: 8–13.

Bird A. 2002. DNA methylation patterns and epigenetic memory. *Genes & Development*, **16**(1): 6–21.

Bommarito PA, Fry RC. 2019. The role of DNA methylation in gene regulation. *In*: Mccullough SD, Dolinoy DC. Toxicoepigenetics: Core Principles and Applications. San Diego: Academic Press, 127–151.

Bossdorf O, Richards CL, Pigliucci M. 2008. Epigenetics for ecologists. *Ecology Letters*, **11**(2): 106–115.

Boyes J, Bird A. 1991. DNA methylation inhibits transcription indirectly via a methyl-CpG binding protein. *Cell*, **64**(6): 1123–1134.

Carbon S, Ireland A, Mungall CJ, et al. 2009. AmiGO: online access to ontology and annotation data. *Bioinformatics*, **25**(2): 288–289.

Chano T, Kita H, Avnet S, et al. 2018. Prominent role of RAB39A-RXRB axis in cancer development and stemness. *Oncotarget*, **9**(11): 9852–9866.

Chapin N, Fernandez J, Poole J, et al. 2022. Anchor-based bisulfite sequencing determines genome-wide DNA methylation. *Communications Biology*, **5**(1): 596.

Chen T, Chen X, Zhang S, et al. 2021. The genome sequence archive family: toward explosive data growth and diverse data types. *Genomics, Proteomics & Bioinformatics*, **19**(4): 578–583.

Chen X, Zhou JR, Li XD, et al. 2018. Exosomes derived from hypoxic epithelial ovarian cancer cells deliver microRNAs to macrophages and elicit a tumor-promoted phenotype. *Cancer Letters*, **435**: 80–91.

Chen YQ, Wu B, Xu LL, et al. 2012. A SNX10/V-ATPase pathway regulates ciliogenesis *in vitro* and *in vivo. Cell Research*, **22**(2): 333–345.

Childebayeva A, Goodrich JM, Leon-Velarde F, et al. 2021. Genome-wide epigenetic signatures of adaptive developmental plasticity in the Andes. *Genome Biology and Evolution*, **13**(2): evaa239.

Childebayeva A, Jones TR, Goodrich JM, et al. 2019. LINE-1 and EPAS1 DNA methylation associations with high-altitude exposure. *Epigenetics*, **14**(1): 1–15.

Chiou KL, Janiak MC, Schneider-Crease IA, et al. 2022. Genomic signatures of high-altitude adaptation and chromosomal polymorphism in geladas. *Nature Ecology & Evolution*, **6**(5): 630–643.

Cho WH, Kang YH, An YY, et al. 2013. Human Tim-Tipin complex affects the biochemical properties of the replicative DNA helicase and DNA polymerases. *Proceedings of the National Academy of Sciences of the United States of America*, **110**(7): 2523–2527.

CNCB-NGDC members & partners. 2021. Database Resources of the National Genomics Data Center, China National Center for Bioinformation in 2022. *Nucleic Acids Research*, **50**(D1): D27–D38.

Corn PG, McDonald III ER, Herman JG, et al. 2003. Tat-binding protein-1, a

component of the 26S proteasome, contributes to the E3 ubiquitin ligase function of the von Hippel-Lindau protein. *Nature Genetics*, **35**(3): 229–237.
Das J. 2006. The role of mitochondrial respiration in physiological and evolutionary adaptation. *BioEssays*, **28**(9): 890–901.
De Souza Iung LH, Mulder HA, de Rezende Neves HH, et al. 2018. Genomic regions underlying uniformity of yearling weight in Nellore cattle evaluated under different response variables. *BMC Genomics*, **19**(1): 619.
Du Q, Luu PL, Stirzaker C, et al. 2015. Methyl-CpG-binding domain proteins: readers of the epigenome. *Epigenomics*, **7**(6): 1051–1073.
Elgendy K, Malcomson FC, Lara JG, et al. 2018. Effects of dietary interventions on DNA methylation in adult humans: systematic review and meta-analysis. *British Journal of Nutrition*, **120**(9): 961–976.
Ettelt R, Vucak G, Didusch S, et al. 2023. Interplay between PLEKHG3-regulated actin dynamics and lysosomal trafficking in cell motility. *bioRxiv*.
Febbraio M, Hajjar DP, Silverstein RL. 2001. CD36: a class B scavenger receptor involved in angiogenesis, atherosclerosis, inflammation, and lipid metabolism. *Journal of Clinical Investigation*, **108**(6): 785–791.
Feil R, Fraga MF. 2012. Epigenetics and the environment: emerging patterns and implications. *Nature Reviews Genetics*, **13**(2): 97–109.
Felfly H, Zambon AC, Xue J, et al. 2011. Severe hypoxia: consequences to neural stem cells and neurons. *Journal of Neurology Research*, **1**(5): 177–189.
Feng H, Tan JN, Wang QJ, et al. 2023. α-hederin regulates glucose metabolism in intestinal epithelial cells by increasing SNX10 expression. *Phytomedicine*, **111**: 154677.
Forester BR, Lasky JR, Wagner HH, et al. 2018. Comparing methods for detecting multilocus adaptation with multivariate genotype-environment associations. *Molecular Ecology*, **27**(9): 2215–2233.
Gambarte Tudela J, Capmany A, Romao M, et al. 2015. The late endocytic Rab39a GTPase regulates the interaction between multivesicular bodies and chlamydial inclusions. *Journal of Cell Science*, **128**(16): 3068–3081.
Gauvreau MÉ, Côté MH, Bourgeois-Daigneault MC, et al. 2009. Sorting of MHC class II molecules into exosomes through a ubiquitin-independent pathway. *Traffic*, **10**(10): 1518–1527.
Geissmann T, Lwin N, Aung SS, et al. 2011. A new species of snub-nosed monkey, genus *Rhinopithecus* Milne-Edwards, 1872 (Primates, Colobinae), from northern Kachin state, northeastern Myanmar. *American Journal of Primatology*, **73**(1): 96–107.
Goonasekera SA, Beard NA, Groom L, et al. 2007. Triadin binding to the C-terminal luminal loop of the ryanodine receptor is important for skeletal muscle excitation-contraction coupling. *Journal of General Physiology*, **130**(4): 365–378.
Govender P, Ghai M, Okpeku M. 2022. Sex-specific DNA methylation: impact on human health and development. *Molecular Genetics and Genomics*, **297**(6): 1451–1466.
Griffis ER, Stuurman N, Vale RD. 2007. Spindly, a novel protein essential for silencing the spindle assembly checkpoint, recruits dynein to the kinetochore. *Journal of Cell Biology*, **177**(6): 1005–1015.
Gugger PF, Fitz-Gibbon S, PellEgrini M, et al. 2016. Species-wide patterns of DNA methylation variation in *Quercus lobata* and their association with climate gradients. *Molecular Ecology*, **25**(8): 1665–1680.
Heijmans BT, Tobi EW, Stein AD, et al. 2008. Persistent epigenetic differences associated with prenatal exposure to famine in humans. *Proceedings of the National Academy of Sciences of the United States of America*, **105**(44): 17046–17049.
Hermes-Lima M, Moreira DC, Rivera-Ingraham GA, et al. 2015. Preparation for oxidative stress under hypoxia and metabolic depression: Revisiting the proposal two decades later. *Free Radical Biology and Medicine*, **89**: 1122–1143.
Hetz C. 2012. The unfolded protein response: controlling cell fate decisions under ER stress and beyond. *Nature Reviews Molecular Cell Biology*, **13**(2): 89–102.
Hibler E, Huang L, Andrade J, et al. 2019. Impact of a diet and activity health promotion intervention on regional patterns of DNA methylation. *Clinical Epigenetics*, **11**(1): 133.
Hidalgo C, Donoso P, Carrasco MA. 2005. The ryanodine receptors Ca^{2+} release channels: cellular redox sensors?. *IUBMB Life*, **57**(4-5): 315–322.
Hilliard AT, Xie D, Ma ZH, et al. 2019. Genome-wide effects of social status on DNA methylation in the brain of a cichlid fish. *Astatotilapia burtoni. BMC Genomics*, **20**(1): 699.
Hoffenberg S, Liu X, Nikolova L, et al. 2000. A novel membrane-anchored rab5 interacting protein required for homotypic endosome fusion. *Journal of Biological Chemistry*, **275**(32): 24661–24669.
Hon GC, Rajagopal N, Shen Y, et al. 2013. Epigenetic memory at embryonic enhancers identified in DNA methylation maps from adult mouse tissues. *Nature Genetics*, **45**(10): 1198–1206.
Horvath S, Haghani A, Macoretta N, et al. 2022. DNA methylation clocks tick in naked mole rats but queens age more slowly than nonbreeders. *Nature Aging*, **2**(1): 46–59.
Hou X, Huang MJ, Zeng XX, et al. 2021. The role of TRPC6 in renal ischemia/reperfusion and cellular hypoxia/reoxygenation injuries. *Frontiers in Molecular Biosciences*, **8**: 698975.
Hou X, Xiao HT, Zhang YH, et al. 2018. Transient receptor potential channel 6 knockdown prevents apoptosis of renal tubular epithelial cells upon oxidative stress via autophagy activation. *Cell Death & Disease*, **9**(10): 1015.
Hu JT, Askary AM, Thurman TJ, et al. 2019. The epigenetic signature of colonizing new environments in *Anolis* lizards. *Molecular Biology and Evolution*, **36**(10): 2165–2170.
Huang J, Gong ZH, Ghosal G, et al. 2009. SOSS complexes participate in the maintenance of genomic stability. *Molecular Cell*, **35**(3): 384–393.
Hubbi ME, Semenza GL. 2015. Regulation of cell proliferation by hypoxia-inducible factors. *American Journal of Physiology-Cell Physiology*, **309**(12): C775–C782.
Huybrechts Y, Van Hul W. 2022. Osteopetrosis associated with *PLEKHM1* and *SNX10* genes, both involved in osteoclast vesicular trafficking. *Bone*, **164**: 116520.
Jarray R, Allain B, Borriello L, et al. 2011. Depletion of the novel protein PHACTR-1 from human endothelial cells abolishes tube formation and induces cell death receptor apoptosis. *Biochimie*, **93**(10): 1668–1675.
Jirtle RL, Skinner MK. 2007. Environmental epigenomics and disease susceptibility. *Nature Reviews Genetics*, **8**(4): 253–262.
Jones PA. 2012. Functions of DNA methylation: islands, start sites, gene bodies and beyond. *Nature Reviews Genetics*, **13**(7): 484–492.
Julian CG, Moore LG. 2019. Human genetic adaptation to high altitude: evidence from the Andes. *Genes* (*Basel*), **10**(2): 150.
Kimura-Ohba S, Yang Y. 2016. Oxidative DNA damage mediated by intranuclear MMP activity is associated with neuronal apoptosis in ischemic stroke. *Oxidative Medicine and Cellular Longevity*, **2016**: 6927328.
Kirkpatrick RC. 1995. The natural history and conservation of the snub-nosed monkeys (genus *Rhinopithecus*). *Biological Conservation*, **72**(3): 363–369.
Krueger F, Andrews SR. 2011. Bismark: a flexible aligner and methylation caller for Bisulfite-Seq applications. *Bioinformatics*, **27**(11): 1571–1572.
Kurien P, Hsu PK, Leon J, et al. 2019. TIMELESS mutation alters phase responsiveness and causes advanced sleep phase. *Proceedings of the National Academy of Sciences of the United States of America*, **116**(24): 12045–12053.
LaBaer J, Garrett MD, Stevenson LF, et al. 1997. New functional activities for the p21 family of CDK inhibitors. *Genes & Development*, **11**(7): 847–862.
Lee FS. 2024. Hypoxia Inducible Factor pathway proteins in high-altitude

mammals. *Trends in Biochemical Sciences*, **49**(1): 79–92.
Leman AR, Dheekollu J, Deng Z, et al. 2012. Timeless preserves telomere length by promoting efficient DNA replication through human telomeres. *Cell Cycle*, **11**(12): 2337–2347.
Lenkov K, Lee MH, Lenkov OD, et al. 2015. Epigenetic DNA methylation linked to social dominance. *PLoS One*, **10**(12): e0144750.
Li BG, Pan RL, Oxnard CE. 2002. Extinction of snub-nosed monkeys in China during the past 400 years. *International Journal of Primatology*, **23**(6): 1227–1244.
Li M, Wei FW, Huang CM, et al. 2004. Phylogeny of snub-nosed monkeys inferred from mitochondrial DNA, cytochrome B, and 12S rRNA sequences. *International Journal of Primatology*, **25**(4): 861–873.
Li PY, Hu XM, Gan Y, et al. 2011. Mechanistic insight into DNA damage and repair in ischemic stroke: exploiting the base excision repair pathway as a model of neuroprotection. *Antioxidants & Redox Signaling*, **14**(10): 1905–1918.
Li Y, Wu DD, Boyko AR, et al. 2014. Population variation revealed high-altitude adaptation of Tibetan mastiffs. *Molecular Biology and Evolution*, **31**(5): 1200–1205.
Liao YH, Erxleben C, Abramowitz J, et al. 2008. Functional interactions among Orai1, TRPCs, and STIM1 suggest a STIM-regulated heteromeric Orai/TRPC model for SOCE/Icrac channels. *Proceedings of the National Academy of Sciences of the United States of America*, **105**(8): 2895–2900.
Liew YJ, Zoccola D, Li Y, et al. 2018. Epigenome-associated phenotypic acclimatization to ocean acidification in a reef-building coral. *Science Advances*, **4**(6): eaar8028.
Lin BL, Shin JY, Jeffreys WPD, et al. 2022. Pharmacological TRPC6 inhibition improves survival and muscle function in mice with Duchenne muscular dystrophy. *JCI Insight*, **7**(19): e158906.
Lisanti S, Omar WAW, Tomaszewski B, et al. 2013. Comparison of methods for quantification of global DNA methylation in human cells and tissues. *PLoS One*, **8**(11): e79044.
Lister R, Pelizzola M, Dowen RH, et al. 2009. Human DNA methylomes at base resolution show widespread epigenomic differences. *Nature*, **462**(7271): 315–322.
Liu D, Zhou D, Sun YF, et al. 2020. A transcriptome-wide association study identifies candidate susceptibility genes for pancreatic cancer risk. *Cancer Research*, **80**(20): 4346–4354.
Logarinho E, Resende T, Torres C, et al. 2008. The human spindle assembly checkpoint protein Bub3 is required for the establishment of efficient kinetochore-microtubule attachments. *Molecular Biology of the Cell*, **19**(4): 1798–1813.
Long YC, Craig K, Zhong T, et al. 1996. Status and conservation strategy of the Yunnan snub-nosed monkey. *Biodiversity Science*, **4**(3): 145–152. (in Chinese)
Long YC, Kirkpatrick CR, Zhong T, et al. 1994. Report on the distribution, population, and ecology of the yunnan snub-nosed monkey (*Rhinopithecus bieti*). *Primates*, **35**(2): 241–250.
Lorenzo FR, Huff C, Myllymäki M, et al. 2014. A genetic mechanism for Tibetan high-altitude adaptation. *Nature Genetics*, **46**(9): 951–956.
Majmundar AJ, Lee DSM, Skuli N, et al. 2015. HIF modulation of Wnt signaling regulates skeletal myogenesis *in vivo. Development*, **142**(14): 2405–2412.
Malumbres M. 2014. Cyclin-dependent kinases. *Genome Biology*, **15**(6): 122.
Mehta RS, Song MY, Nishihara R, et al. 2017. Dietary patterns and risk of colorectal cancer: analysis by tumor location and molecular subtypes. *Gastroenterology*, **152**(8): 1944–1953. e1.
Moarii M, Boeva V, Vert JP, et al. 2015. Changes in correlation between promoter methylation and gene expression in cancer. *BMC Genomics*, **16**: 873.
Mohn F, Schübeler D. 2009. Genetics and epigenetics: stability and plasticity during cellular differentiation. *Trends in Genetics*, **25**(3): 129–136.
Moleirinho A, Lopes AM, Seixas S, et al. 2015. Distinctive patterns of evolution of the *δ-globin* gene (HBD) in primates. *PLoS One*, **10**(4): e0123365.
Naimi B, Hamm NAS, Groen TA, et al. 2014. Where is positional uncertainty a problem for species distribution modelling?. *Ecography*, **37**(2): 191–203.
Nakaya M, Kitano M, Matsuda M, et al. 2008. Spatiotemporal activation of Rac1 for engulfment of apoptotic cells. *Proceedings of the National Academy of Sciences of the United States of America*, **105**(27): 9198–9203.
Nizet V, Johnson RS. 2009. Interdependence of hypoxic and innate immune responses. *Nature Reviews Immunology*, **9**(9): 609–617.
O'Donnell L, Panier S, Wildenhain J, et al. 2010. The MMS22L-TONSL complex mediates recovery from replication stress and homologous recombination. *Molecular Cell*, **40**(4): 619–631.
Oksanen J, Simpson GL, Blanchet FG, et al. 2022. vegan: community ecology package.
Pal A, Srivastava T, Sharma MK, et al. 2010. Aberrant methylation and associated transcriptional mobilization of *Alu* elements contributes to genomic instability in hypoxia. *Journal of Cellular and Molecular Medicine*, **14**(11): 2646–2654.
Palomera-Sanchez Z, Zurita M. 2011. Open, repair and close again: chromatin dynamics and the response to UV-induced DNA damage. *DNA Repair*, **10**(2): 119–125.
Pankiv S, Alemu EA, Brech A, et al. 2010. FYCO1 is a Rab7 effector that binds to LC3 and PI3P to mediate microtubule plus end-directed vesicle transport. *Journal of Cell Biology*, **188**(2): 253–269.
Patel RK, Jain M. 2012. NGS QC Toolkit: a toolkit for quality control of next generation sequencing data. *PLoS One*, **7**(2): e30619.
Pizzo P, Pozzan T. 2007. Mitochondria-endoplasmic reticulum choreography: structure and signaling dynamics. *Trends in Cell Biology*, **17**(10): 511–517.
Pollice A, Vivo M, La Mantia G. 2008. The promiscuity of ARF interactions with the proteasome. *FEBS Letters*, **582**(23-24): 3257–3262.
Prentki M, Madiraju SRM. 2008. Glycerolipid metabolism and signaling in health and disease. *Endocrine Reviews*, **29**(6): 647–676.
Pugh CW, Ratcliffe PJ. 2003. Regulation of angiogenesis by hypoxia: role of the HIF system. *Nature Medicine*, **9**(6): 677–684.
Qin BM, He M, Chen X, et al. 2006. Sorting nexin 10 induces giant vacuoles in mammalian cells. *Journal of Biological Chemistry*, **281**(48): 36891–36896.
Richards EJ. 2006. Inherited epigenetic variation — revisiting soft inheritance. *Nature Reviews Genetics*, **7**(5): 395–401.
Ridley AJ, Paterson HF, Johnston CL, et al. 1992. The small GTP-binding protein rac regulates growth factor-induced membrane ruffling. *Cell*, **70**(3): 401–410.
Rosales C, Uribe-Querol E. 2017. Phagocytosis: a fundamental process in immunity. *BioMed Research International*, **2017**: 9042851.
Rouschop KMA, van den Beucken T, Dubois L, et al. 2010. The unfolded protein response protects human tumor cells during hypoxia through regulation of the autophagy genes *MAP1LC3B* and *ATG5. Journal of Clinical Investigation*, **120**(1): 127–141.
Salameh Y, Bejaoui Y, El Hajj N. 2020. DNA methylation biomarkers in aging and age-related diseases. *Frontiers in Genetics*, **11**: 171.
Salceda S, Caro J. 1997. Hypoxia-inducible factor 1α (HIF-1α) protein is rapidly degraded by the ubiquitin-proteasome system under normoxic conditions. Its stabilization by hypoxia depends on redox-induced changes. *Journal of Biological Chemistry*, **272**(36): 22642–22647.
Schübeler D. 2015. Function and information content of DNA methylation. *Nature*, **517**(7534): 321–326.
Schüchner S, Tembe V, Rodriguez JA, et al. 2005. Nuclear targeting and

cell cycle regulatory function of human BARD1. *Journal of Biological Chemistry*, **280**(10): 8855–8861.
Semenza GL. 2011. Hypoxia. Cross talk between oxygen sensing and the cell cycle machinery. *American Journal of Physiology-Cell Physiology*, **301**(3): C550–C552.
Semenza GL. 2012. Hypoxia-inducible factors in physiology and medicine. *Cell*, **148**(3): 399–408.
Shahrzad S, Bertrand K, Minhas K, et al. 2007. Induction of DNA hypomethylation by tumor hypoxia. *Epigenetics*, **2**(2): 119–125.
Simonson TS, Yang YZ, Huff CD, et al. 2010. Genetic evidence for high-altitude adaptation in Tibet. *Science*, **329**(5987): 72–75.
Smith ZD, Meissner A. 2013. DNA methylation: roles in mammalian development. *Nature Reviews Genetics*, **14**(3): 204–220.
Somyajit K, Gupta R, Sedlackova H, et al. 2017. Redox-sensitive alteration of replisome architecture safeguards genome integrity. *Science*, **358**(6364): 797–802.
Song K, Gao B, Halvarsson P, et al. 2022. Conservation genomics of sibling grouse in boreal forests reveals introgression and adaptive population differentiation in genes controlling epigenetic variation. *Zoological Research*, **43**(2): 184–187.
Song S, Yao N, Yang M, et al. 2016. Exome sequencing reveals genetic differentiation due to high-altitude adaptation in the Tibetan cashmere goat (*Capra hircus*). *BMC Genomics*, **17**: 122.
Sultana F, Morse LR, Picotto G, et al. 2020. Snx10 and PIKfyve are required for lysosome formation in osteoclasts. *Journal of Cellular Biochemistry*, **121**(4): 2927–2937.
Susan JC, Harrison J, Paul CL, et al. 1994. High sensitivity mapping of methylated cytosines. *Nucleic Acids Research*, **22**(15): 2990–2997.
Suzuki M, Liao W, Wos F, et al. 2018. Whole-genome bisulfite sequencing with improved accuracy and cost. *Genome Research*, **28**(9): 1364–1371.
Szpiech ZA, Novak TE, Bailey NP, et al. 2021. Application of a novel haplotype-based scan for local adaptation to study high-altitude adaptation in rhesus macaques. *Evolution Letters*, **5**(4): 408–421.
Topolska-Woś AM, Chazin WJ, Filipek A. 2016. CacyBP/SIP — structure and variety of functions. *Biochimica et Biophysica Acta (BBA) - General Subjects*, **1860**(1): 79–85.
Ulahannan N, Greally JM. 2015. Genome-wide assays that identify and quantify modified cytosines in human disease studies. *Epigenetics & Chromatin*, **8**: 5.
Ünsal-Kaçmaz K, Chastain PD, Qu PP, et al. 2007. The human Tim/Tipin complex coordinates an Intra-S checkpoint response to UV that slows replication fork displacement. *Molecular and Cellular Biology*, **27**(8): 3131–3142.
Walbrecq G, Lecha O, Gaigneaux A, et al. 2020. Hypoxia-induced adaptations of miRNomes and proteomes in melanoma cells and their secreted extracellular vesicles. *Cancers*, **12**(3): 692.
Wang CW, Klionsky DJ. 2003. The molecular mechanism of autophagy. *Molecular Medicine*, **9**(3-4): 65–76.
Wang X, Ni JH, You Y, et al. 2021. SNX10-mediated LPS sensing causes intestinal barrier dysfunction via a caspase-5-dependent signaling cascade. *The EMBO Journal*, **40**(24): e108080.
Wang Y, Li XH, Duan HZ, et al. 2009. Altered stored calcium release in skeletal myotubes deficient of triadin and junctin. *Cell Calcium*, **45**(1): 29–37.
Wang YX, Zheng YM. 2010. ROS-dependent signaling mechanisms for hypoxic Ca^{2+} responses in pulmonary artery myocytes. *Antioxidants & Redox Signaling*, **12**(5): 611–623.
Watt F, Molloy PL. 1988. Cytosine methylation prevents binding to DNA of a HeLa cell transcription factor required for optimal expression of the adenovirus major late promoter. *Genes & Development*, **2**(9): 1136–1143.
Wei C, Wang H, Liu G, et al. 2016. Genome-wide analysis reveals adaptation to high altitudes in Tibetan sheep. *Scientific Reports*, **6**(1): 26770.
Williams BR, Miller AJ, Edwards CE. 2023. How do threatened plant species with low genetic diversity respond to environmental stress? Insights from comparative conservation epigenomics and phenotypic plasticity. *Molecular Ecology Resources*, doi: 10.1111/1755-0998.13897.
Xie S, Mortusewicz O, Ma HT, et al. 2015. Timeless interacts with PARP-1 to promote homologous recombination repair. *Molecular Cell*, **60**(1): 163–176.
Xue Y, Bi F, Zhang XY, et al. 2006. Role of Rac1 and Cdc42 in hypoxia induced p53 and von Hippel-Lindau suppression and HIF1α activation. *International Journal of Cancer*, **118**(12): 2965–2972.
You WK, McDonald DM. 2008. The hepatocyte growth factor/c-Met signaling pathway as a therapeutic target to inhibit angiogenesis. *BMB Reports*, **41**(12): 833–839.
Yu GC, Wang LG, Han YY, et al. 2012. clusterProfiler: an R package for comparing biological themes among gene clusters. *OMICS: A Journal of Integrative Biology*, **16**(5): 284–287.
Yu L, Wang GD, Ruan J, et al. 2016. Genomic analysis of snub-nosed monkeys (*Rhinopithecus*) identifies genes and processes related to high-altitude adaptation. *Nature Genetics*, **48**(8): 947–952.
Yu L, Wang XP, Ting N, et al. 2011. Mitogenomic analysis of Chinese snub-nosed monkeys: Evidence of positive selection in NADH dehydrogenase genes in high-altitude adaptation. *Mitochondrion*, **11**(3): 497–503.
Zaghlool SB, Al-Shafai M, Al Muftah WA, et al. 2015. Association of DNA methylation with age, gender, and smoking in an Arab population. *Clinical Epigenetics*, **7**(1): 6.
Zeng T, Yin JM, Feng PS, et al. 2022. Analysis of genome and methylation changes in Chinese indigenous chickens over time provides insight into species conservation. *Communications Biology*, **5**(1): 952.
Zeng YD, Qin T, Flamini V, et al. 2020. Identification of DHX36 as a tumour suppressor through modulating the activities of the stress-associated proteins and cyclin-dependent kinases in breast cancer. *American Journal of Cancer Research*, **10**(12): 4211–4233.
Zhang B, Ban DM, Gou X, et al. 2019. Genome-wide DNA methylation profiles in Tibetan and Yorkshire pigs under high-altitude hypoxia. *Journal of Animal Science and Biotechnology*, **10**: 25.
Zhao J, Mialki RK, Wei JX, et al. 2013. SCF E3 ligase F-box protein complex SCF^{FBXL19} regulates cell migration by mediating Rac1 ubiquitination and degradation. *The FASEB Journal*, **27**(7): 2611–2619.
Zhao M, Zhang RZ, Qi DW, et al. 2020. CacyBP/SIP promotes tumor progression by regulating apoptosis and arresting the cell cycle in osteosarcoma. *Experimental and Therapeutic Medicine*, **20**(2): 1397–1404.
Zhao XH, Lasell TKR, Melancİon P, et al. 2002. Localization of large ADP-ribosylation factor-guanine nucleotide exchange factors to different Golgi compartments: evidence for distinct functions in protein traffic. *Molecular Biology of the Cell*, **13**(1): 119–133.
Zhou XM, Meng XH, Liu ZJ, et al. 2016. Population genomics reveals low genetic diversity and adaptation to hypoxia in snub-nosed monkeys. *Molecular Biology and Evolution*, **33**(10): 2670–2681.
Zhou XM, Wang BS, Pan Q, et al. 2014. Whole-genome sequencing of the snub-nosed monkey provides insights into folivory and evolutionary history. *Nature Genetics*, **46**(12): 1303–1310.
Ziller MJ, Gu HC, Müller F, et al. 2013. Charting a dynamic DNA methylation landscape of the human genome. *Nature*, **500**(7463): 477–481.